Int J Adv Manuf Technol (2012) 62:89–97
DOI 10.1007/s00170-011-3779-3

ORIGINAL ARTICLE

The avoidance of cutter gouging in five-axis machining with a fillet-end milling cutter

Juan Du · Xian-guo Yan · Xi-tian Tian

Received: 6 January 2011 / Accepted: 14 November 2011 / Published online: 13 December 2011

Abstract This paper proposes a new method of automatic detection and elimination of cutter gouging when using the fillet-end milling cutter to produce a complex surface on the five-axis computer numerical control machine tool. To avoid local cutter gouging at the point where the cutter and part surface make contact with each other, the method of exact curvature matching between the cutter and part surface is presented. The size of cutter radii is more easily determined by this method. To detect if a rear cutter gouging occurs near the contact point, a square grid with horizontal and vertical points is used for illustrating the checking area and checking points. The technique of automatic generation of the square grid points and the method of detection and avoidance of rear cutter gouging are investigated throughout this article. In the end, the studied methodology and algorithms are inspected and verified by using an example of nonuniform rational B spline surface.

Keywords Five-axis machining · Fillet-end milling cutter · Cutter gouging · Exact curvature matching · Square grid points

J. Du (✉) · X.-g. Yan
School of Electromechanic,
Taiyuan University of Science & Technology,
Taiyuan 030024, China
e-mail: china_azalea@163.com

X.-t. Tian
School of Electromechanic,
Northwestern Polytechnical University,
Xian 710072, China

1 Introduction and literature review

Complex surfaces are widely used today in aerospace, automobile, and the tool and die manufacturing industries. These surfaces are frequently made by a three-axis computer numerical control (CNC) milling machine using a ball-end milling cutter in most cases. A ball-end cutter is easier to orient itself relative to a surface and generate simple NC programs; however, the machining efficiency is very low. Due to the two additional rotational motions, five-axis machining has more advantages than three-axis machining, such as faster material removal rates and an improved accuracy and surface finish [1–4]. This technique gives machinery greater flexibility in making parts that have complex surfaces. Five-axis CNC machine tools are more and more widely used in modern manufacturing.

Cutter gouging avoidance is a major determining factor for using the five-axis machine tool to produce higher quality complex surface. Therefore, the purpose of this paper and its main focus is to illustrate how to avoid this problem in the five-axis machining of complex surface when using a fillet-end milling cutter. Cutter gouging refers to the removal of the excess material in the vicinity of the cutter contact point, hereafter referred to as simply CCP, and as a result of disparity in curvature between the cutter surface and the part surface or the improper orientation of the cutter relative to the part surface [5]. To achieve a gouge-free cutter path, many algorithms were developed for cutter gouging avoidance [6–16]. Several studies proposed that a correct cutter orientation be determined based on curvature matching between the cutter and machined surface through the application of differential geometrical technique [6, 7, 12]. This technique has been applied to detect local cutter gouging by comparing the valid cutting radius of the cutter with the curvature radius of the part

surface on the plane that is perpendicular to the tool path and passing through the CCP, and local cutter gouging at the CCP can be reduced and eliminated by changing the inclination and tilt angle of the cutter [13–16]. Chen et al. also presented a way of avoidance of cutter local gouging by considering curvature matching between cutter and part surface on the osculation plane through the CCP [17]. A similar hypothesis by Lee [18] and Than [5] suggests that a proper inclination angle of the cutter can be found by taking into account the effective cutting radius on tangent plane and normal plane of the CCP. The above methods based on curvature matching did not consider the curvature variation of the cutter surface and the part surface in all directions with the exceptions of the one that is perpendicular to or parallel to the tool path. Rear gouging or rear interference, as it is also known, happens at the adjacent area of the CCP and was unfortunately neglected by all of them in their studies of cutter gouging. Therefore, the relative movement between cutter and part surface was not accurately portrayed through their analysis of curvature matching by consideration of only on one or two planes [19].

Another general method of checking cutter gouging is to use the distance between the bottom of cutter and the part surface to determine if a cutter gouging occurs [20–24]. To make simple computation of distance, the part surface needs to be separated into a large number of triangular facets first; and the distance between the cutter bottom and the part surface is replaced with the thought of the distance between the cutter bottom and the triangular facet. Another cutter gouging detection method proposed by Jensen and Anderson [25] uses polynomial resultants to calculate intersection conditions between the bottom of the cutter and a lower profile tolerance surface offset of the part. Cutter interference (gouging) will come about at any point of intersection. Their method based on distance or intersection conditions is much too complicated and time consuming. Most researchers have only placed particular emphasis on the algorithm of checking and avoidance of cutter gouging. However, the method of triangle facet discretion used by them for automatic generation of checking points was not provided in complete detail. Ahmet [26] proposed a method based on parameter domain for automatic generating checking area and checking points. In his study, the detection of cutter gouging was done by computing the maximum inclination angle of the line joining the CCP and the checking point with respect to the bottom plane of the cutter.

In this study, cutter gouging is classified into two types: local curvature interference at contact point and rear interference. Local curvature interference arises when the curvature of the cutter surface is smaller than curvature of the part surface at the CCP; rear interference results from improper tool orientation as shown in Fig. 1. Fillet-end

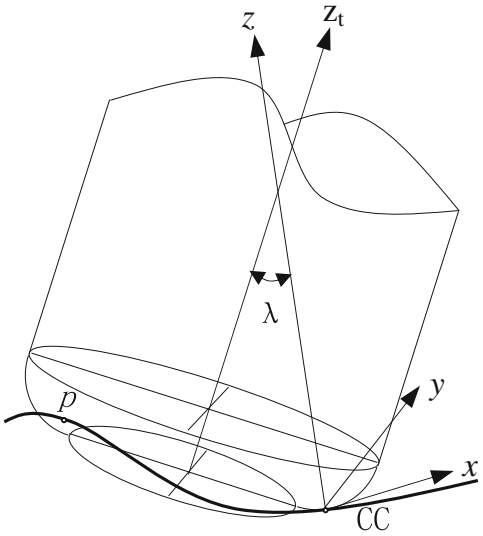

Fig. 1 Rear interference

milling cutter is in wide usage today along with the five-axis machining because it has the virtue of good performance and wearing resistance. Unlike the flat end milling cutter, its work area is a torus surface. Local curvature interference may be occurring in any direction on the tangent plane of the CCP. An effective searching algorithm was developed for automatic determination of cutter radii as a way to avoid local curvature interference. The technique of detection and avoidance of rear interference is given in detail in the following text.

2 Five-axis machining and the associated coordinate systems

The basic concepts of five-axis machining with a fillet-end milling cutter and coordinate systems are illustrated in Fig. 2. The global coordinate system is defined by (X, Y, Z) and the symbol Σ denotes machined surface (r [u (t), v (t)]).

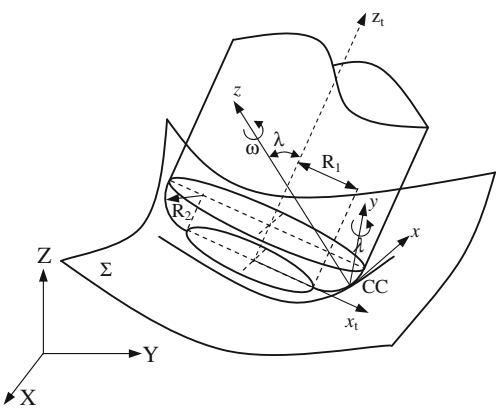

Fig. 2 Five-axis machining and the associate coordinate systems

Local coordinate system is established at the CCP on the part surface by (CC, x, y, z), where x-axis is in the direction of tool motion and z-axis is parallel to the normal direction of the CCP, and so $y = z \times x$. Tool coordinate system is build using the center of bottom circle of the fillet-end cutter as the origin of coordinate and the axis of cutter is used as z_t. The x_t originates from the origin of coordinate and is along the tangent of x-axis when the tool tilt angle is set to 0. Tool movement trajectory in five-axis is expressed by tool location points (X, Y, Z) in the work piece coordinate and tool orientation that is established by the inclination angle and tilt angles. The cutter is first rotated about y for an inclination angle λ and then about z for a tilt angle ω. In general, $0 \le \lambda \le 90°$ and $-90° \le \omega \le 90°$.

2.1 Cutter gouging detection and avoidance

There are two steps in this approach. At the first stage, according to the method of exact curvature machining, the proper size of cutter radii is selected for the avoidance of the local curvature interference, and the minimum initial inclination angle of the cutter is determined at each CCP. At the second stage, the rear interference is detected and corrected, and the final cutter inclination angle is found for avoidance of rear interference as well as local curvature interference.

2.2 Avoidance of local curvature interference

In order to obtain exact curvature matching between the cutter part and the surface at the CCP, two principal curvatures of the cutter surface and the part surface must first be calculated.

2.2.1 Calculation of the principal curvature for cutter surface and part surface

A surface with $|r_u \times r_v| \neq 0$ is called regular surface, where r_u and r_v are two tangent vectors of the parametric surface. Two principal curvatures of surface, also termed the maximum normal curvature K_{max} and the minimum normal curvature K_{min}, can be given by the following equation.

$$(EG - F^2)k^2 - (EN - 2FM + GL)k + (LN - M^2) = 0 \tag{1}$$

In the above equation, E, F, and G are the first fundamental elements of the machined surface, and L, M, and N are the second fundamental elements. They are given as follows:

$$\begin{array}{llll} E = r_u^2 & F = r_u \cdot r_v & G = r_v^2 & L = n \cdot r_{uu} = -n_u \cdot r_u \\ M = n \cdot r_{uv} = -n_u \cdot r_v = -n_v \cdot r_u & N = n \cdot r_{vv} = -n_v \cdot r_v & n \frac{r_u \times r_v}{|r_u \times r_v|} & \end{array} \tag{2}$$

where n is the unit normal vector of the machined surfaced and subscripts indicate differentiation with respect to the subscripted value. When the CCP is known, the E, F, G, L, M, and N can be worked out using the equations above. Therefore, two different solutions of Eq. 1 can be solved, and the values of two solutions correspond to the maximum principal curvature K_{max} and the minimum normal curvature K_{min} of the surface at the CCP, respectively.

The working surface of fillet-end milling cutter is a standard surface of revolution, indicating the first principal direction corresponding to the maximum principal curvature being tangent to the meridian of the cutter according to differential geometry; the second principal direction is tangent to the latitude of the cutter. In accordance with the Meusnier's theory, the maximum principal curvature k_{max} and the minimum principal curvature k_{min} of the cutter working surface can be obtained with the equations listed below.

$$k_{max} = \frac{1}{R^2} \qquad k_{min} = \frac{\sin\lambda}{R_1 + R_2 \sin\lambda} \tag{3}$$

where R_1 is the radius of bottom circle of cutter, and R_2 is the cutter fillet radius as shown in Fig. 2, and λ is the inclination angle of cutter.

2.2.2 Selection of cutter radius

Local curvature interference is due to mismatch in the curvature between the cutter working surface and the part surface at the CCP in some directions. To keep from local curvature interference at each CCP, the minimum principal curvature of the cutter has to be equal to or greater than the maximum principal curvature of the surface to be machined.

The maximum principal curvature of part surface is constant value for each CCP while the minimum principal curvature of the cutter working surface does not depend on the cutter radii R_1 and R_2, but also on the inclination angle λ according to the Eq. 3. Local curvature interference at the CCP can be eliminated when the size of the cutter radii is accurately selected before machining is initiated.

The shape type of the machined surface must be decided by the signs of two principal curvatures at the CCP before selection of the cutter radius value. The signs of K_{max} and K_{min} depend on the direction of normal vector of machined surface at CCP. This research used the positive normal vector direction of the part surface as being the one that conforms to the positive direction of axis Z of the global coordinating system and giving way to the part surface that is convex at the CCP, as the signs of two principal curvatures are negative. Conversely, it is concave at the CCP with the exception of the abovementioned geometric state.

If the part surface is convex at the CCP, there is no occurrence of local curvature interference. Local curvature

interference may happen at the concave surface. The size of the cutter radii depends on the minimum principal curvature radius of the concave surface. The minimum principal curvature of the cutter working surface must be equal to or greater than the maximum principal of the concave surface to be machined. Equation 3 illustrates the larger inclination angle λ, the larger minimum principal curvature of the cutter. Universally, the inclination angle is chosen by acknowledgment of the fact that the smaller the size of the inclination angle is, the better the results of ensuring a larger path interval is employed thus improving machining effectiveness and operation. However, a decrease in the size of the tool inclination angle also reduces proportionally the minimum principal curvature of the cutter but does increase the possibility of local curvature interference and rear interference in practical machining.

Inclination angle is chosen for the selection of the tool radii value according to the shape of the part surface. Given a reasonable inclination angle λ_0, the size of the cutter radii R_1 and R_2 can be calculated using the following equation:

$$k_{\min} = \frac{\sin\lambda_0}{R_1 + R_2 \sin\lambda_0} = K_{\Sigma\max} \tag{4}$$

where the $K_{\Sigma\max}$ is the maximum principal curvature of the concave surface to be machined. Because there are two unknown variables in the equation cited above, the size of cutter radii R_1 and R_2 will be obtained by applying an iterative method as shown in Fig. 3. As the size of cutter radii is determined by the maximum principal curvature $K_{\Sigma\max}$ of the concave surface, for the other CCP on the concave surface where the maximum principal curvature

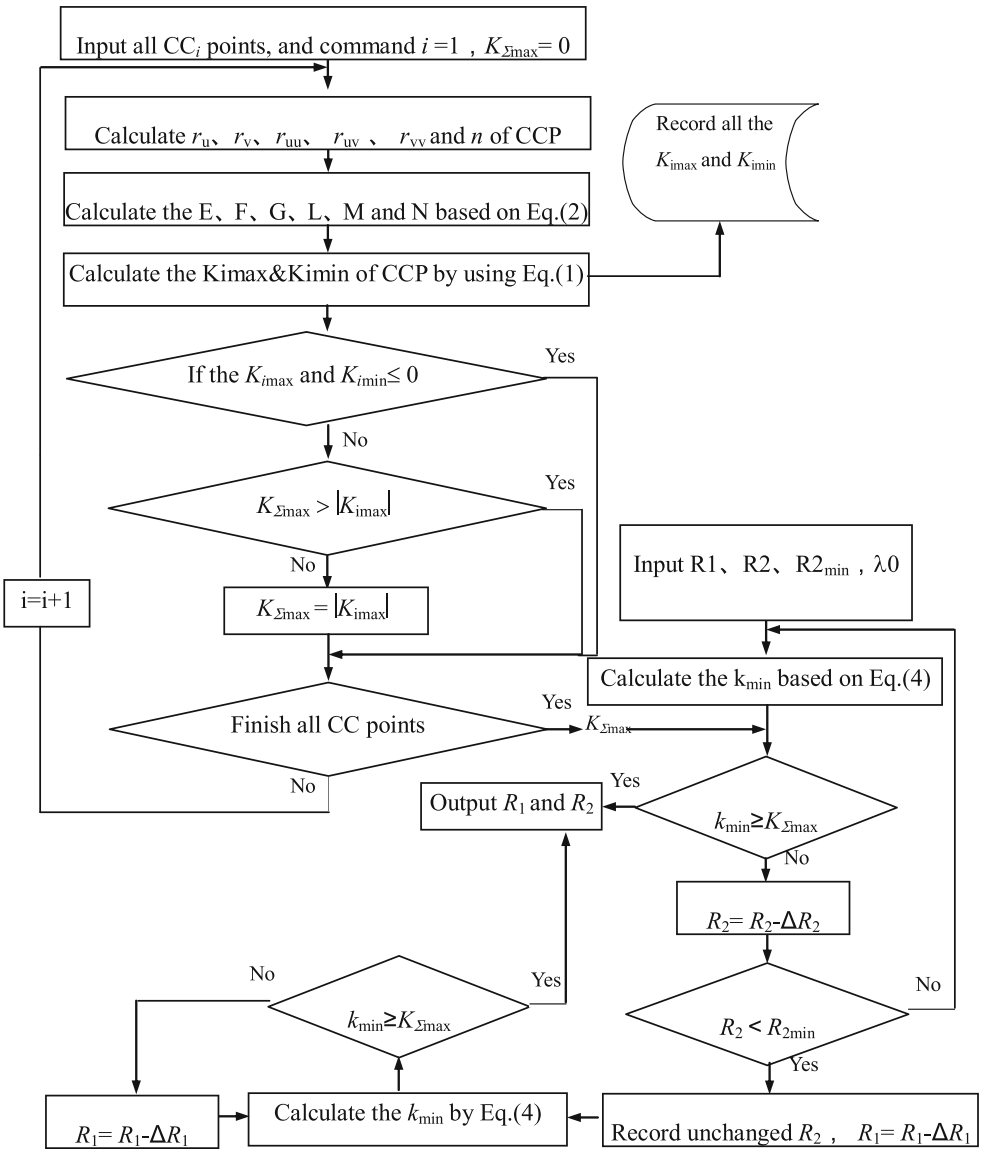

Fig. 3 A flow chart for automatic selection algorithm of cutter radius

is smaller than the $K_{\Sigma max}$, the tool inclination angle λ will be smaller than λ_0 according to Eq. 4, indicating the highest potential for machining efficiency can be achieved by using a smaller inclination angle of the cutter at those cutter contact points.

2.2.3 Detection and avoidance of local curvature interference

Tool inclination angle is one of decisive factors in machining efficiency, while the angle of tilt is the main concern for symmetry of the cutting ellipse and the maximum side site is obtainable when the tilt angle reaches 0. The angle of the tilt has traditionally been fixed to a degree of 0 in most scientific studies [4, 11, 26, 27]. The angle λ_1 set to 5° is used as the minimum inclination angle for the convex surface to reach and maintain a high level of efficiency. Local curvature interference has to be detected and eliminated if the surface is concave at the CCP. Minimum principal curvature of the cutter is calculated by minimum inclination angle λ_1, and then the minimum principal curvature of the cutter is compared to the maximum principal curvature of the concave surface. As the minimum principal curvature of the cutter is equal to or greater than the maximum principal curvature of the concave surface, 5^0 is the initial inclination angle λ_1 that ensures no local interference at the CCP. Otherwise, the initial inclination angle should be increased until the minimum principal curvature of the cutter becomes equal to or greater than the maximum principal curvature of the part surface.

2.3 Rear interference detection and elimination

2.3.1 Checking area and checking point

Determination of the checking area and checking points are the first priority to test out whether rear interference (rear gouging) arises in the vicinity of the CCP. The assumption and precondition for the tool shadow on the part surface is that it be should a circle. To guarantee the shadow of the cutter on the part surface is in the checking area, square grid points are employed establishing the checking area and checking points. The length of the square edge is hypothetical as shown in $2(R_1+R_2)$. The points $P_{0,\ j}(u,\ v)$ (j=1,2,…,m) that are denoted by the furcated sign as given in Fig. 4 are discovered away from the CCP $P_{0,0}(u_0,\ v_0)$ in the opposite direction of the cutter feed. As the point interval is given by Δl, the $m=2(R_1+R_2)/\Delta l$. When all points $P_{0,\ j}(u,\ v)$ are found, it is still necessary to continue searching for points $P_{i,j}(i=\pm1,\ \pm2,\ \ldots,\ \pm n)$ that are situated on the same column as point $P_{0,\ j}$, the columns must lie in a path perpendicular to the direction of cutter feed. The value

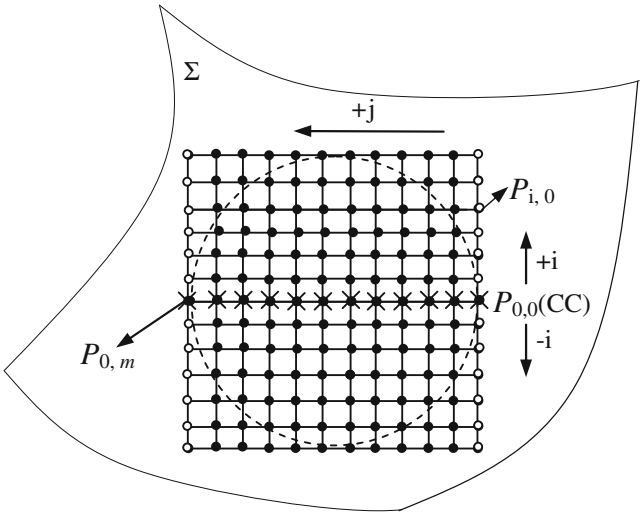

Fig. 4 Checking area and checking points

of n is equal to $(R_1+R_2)/\Delta l$. The smaller the Δl, the greater the probability there is for precision in detection of rear gouging.

When the $r_{0,0}(u_0,\ v_0)$ is the radial vector of point $P_{0,0}$, and the $r_{0,j}(u,\ v)$ is the radial vector of point $P_{0,\ j}$, then the point $P_{0,\ j}$ can be determined using the equations below:

$$\begin{cases} \left|r_{0,j}(u,v)-r_{0,0}(u_0,v_0)\right|_{Z=0} & =\Delta l\cdot j \\ \left.\frac{r_{0,0}(u_0,v_0)-r_{0,j}(u,v)}{\left|r_{0,0}(u_0,v_0)-r_{0,j}(u,v)\right|}\right|_{Z=0} & =\left.\frac{r_t(u_0,v_0)}{|r_t(u_0,v_0)|}\right|_{Z=0} \end{cases} \quad (j=1,2,\ldots m) \tag{5}$$

In the above equations, the $r_t(u_0,\ v_0)$ is shown to be the direction vector of the tool feed and can be substituted by the tangent vector of the tool path curve at the CCP. The radial vector $r_{i,\ j}(u,\ v)$ of the point $P_{i,j}$ is known by the point $P_{0,\ j}$. Progressive checking efficiency is done only through computation of the black dots on the square grid used as an illustration below, while the white dots are to be ignored. The radial vector $r_{i,\ j}(u,\ v)$ of the black points $P_{i,\ j}$ can be computed with the following equations:

$$\begin{cases} \left|r_{i,j}(u,v)-r_{0,j}(u,v)\right|_{Z=0}=\Delta l\cdot|i| \\ \left[r_{i,j}(u,v)-r_{o,j}(u,v)\right]\cdot r_t(u_0,v_0)=0 \\ (i=\pm1,\pm2,\ldots,\pm n;j=1,2,\ldots,m-1) \end{cases} \tag{6}$$

By using Eqs. 5 and 6, the black dots on the square grid can be perceived and utilized as the initial checking point. The cutter shadow on the part surface will be an ellipse with a long radius of the sum of R_1 and R_2 when the inclination angle of the cutter is not equal to 0. To ensure all points in the elliptical shadow are included in the circular area, the ellipse shadow is replaced by a circle and the radius of the circular area has to be equal to the long radius of the ellipse. A dashed circle is used to show

the border of the circular shadow on the part surface in Fig. 4. Continuing with Fig. 4, it is obvious that the majority of the black dots on the square grid are embodied within the circle. And only a few of the black dots, displayed in Fig. 4, are outside of the circle. The use of those black points located in the circle can be viewed as the final valid checking points for rear gouging detection. Thus, the selection of valid checking points from the initial checking points should be carried out before rear gouging detection.

2.3.2 Selection of valid checking points

Valid checking points are those that lie in the circular shadow on the part surface. To determine whether a black point on the square grid is valid checking point, transformation of the points on the part surface in the global coordinate system into the tool coordinate system is a priority for distinguishing of valid checking points. The coordinate transform matrix is depicted below:

$$M_{\mathrm{TM}} = M_{\mathrm{TL}} \cdot M_{\mathrm{LM}} = (M_{\mathrm{LT}})^{-1} \cdot (M_{\mathrm{ML}})^{-1} \tag{7}$$

where the M_{TM} is transform matrix from global coordinate system to tool coordinate system, M_{TL} is transform matrix from local coordinate system to tool coordinate system, and M_{LM} is transform matrix from global coordinate system to local coordinate system. With the relations between the three coordinate systems shown in Fig. 2, the M_{TM} can be expressed as follows:

$$M_{\mathrm{TM}} = \begin{bmatrix} 1 & 0 & 0 & R_1 + R_2 \sin\lambda \\ 0 & 1 & 0 & 0 \\ 0 & 0 & 1 & R_2(1-\cos\lambda) \\ 0 & 0 & 0 & 1 \end{bmatrix} \begin{bmatrix} \cos\lambda & 0 & -\sin\lambda & 0 \\ 0 & 1 & 0 & 0 \\ \sin\lambda & 0 & \cos\lambda & 0 \\ 0 & 0 & 0 & 1 \end{bmatrix} \begin{bmatrix} \cos\omega & \sin\omega & 0 & 0 \\ -\sin\omega & \cos\omega & 0 & 0 \\ 0 & 0 & 1 & 0 \\ 0 & 0 & 0 & 1 \end{bmatrix} \begin{bmatrix} a_{11} & a_{12} & a_{13} & -r_{0X} \\ a_{21} & a_{22} & a_{23} & -r_{0Y} \\ a_{31} & a_{32} & a_{33} & -r_{0Z} \\ 0 & 0 & 0 & 1 \end{bmatrix} \tag{8}$$

Where $[a_{11}\ a_{12}\ a_{13}] = \frac{r_t}{|r_t|}$, $[a_{31}\ a_{32}\ a_{33}] = n = \frac{r_u \times r_v}{|r_u \times r_v|}$, and $[a_{21}\ a_{22}\ a_{23}] = n \times \frac{r_t}{|r_t|}$. The $r_{0,0}(u_0,v_0)$ is the radial vector of the CC point, and the r_{0x},r_{0y} and r_{0Z} are X, Y, and Z vectors of $r_{0,0}(u_0,v_0)$ in the global coordinates system, respectively. When the radial vector r of the point P on the part surface is represented as $r = [r_X,r_Y,r_Z]$ in global coordinates, the corresponding point $P_t(x_t, y_t, z_t)$ in the tool coordinates system can be obtained from the following equation:

$$[x_t\ y_t\ z_t\ 1]^{-1} = M_{\mathrm{TM}} \cdot [r_X\ r_Y\ r_Z]^{-1} \tag{9}$$

When the initial inclination angle of the tool at the CCP is λ_1 and the tilt angle is set to 0 (ω=0°), as Eq. 8 indicates that Eq. 9 is expressed in the following formula:

$$\begin{bmatrix} x_t \\ y_t \\ Z_t \\ 1 \end{bmatrix} = \begin{bmatrix} m_1 r_X + m_2 r_Y + m_3 r_Z + m_4 \\ a_{21} r_X + a_{22} r_Y + a_{23} r_Z - r_{0Y} \\ n_1 r_X + n_2 r_Y + n_3 r_Z + n_4 \\ 1 \end{bmatrix} \tag{10}$$

where,

$$\begin{aligned} m_1 &= a_{11}\cos\lambda_1 - a_{31}\sin\lambda_1 \\ m_2 &= a_{12}\cos\lambda_1 - a_{32}\sin\lambda_1 \\ m_3 &= a_{13}\cos\lambda_1 - a_{33}\sin\lambda_1 \\ m_4 &= -r_{0x}\cos\lambda_1 + r_{0z}\sin\lambda_1 + R_1 + R_2\sin\lambda_1 \\ n_1 &= a_{11}\sin\lambda_1 + a_{31}\cos\lambda_1 \\ n_2 &= a_{12}\sin\lambda_1 + a_{32}\cos\lambda_1 \\ n_3 &= a_{13}\sin\lambda_1 + a_{33}\cos\lambda_1 \\ n_4 &= -r_{0x}\sin\lambda_1 - r_{0Y}\sin\lambda_1 - r_{0z}\cos\lambda_1 + R_2(1-\cos\lambda_1) \end{aligned}$$

Transformation from the initial checking point to its corresponding point in the tool coordinate system is accomplished by using Eq. 10; when the corresponding point is expressed as P_t (x_t,y_t,z_t), the condition for the black dot on the square grid lying in the circular shadow can be realized with the formula given below:

$$x_t^2 + y_t^2 \le (R_1 + R_2)^2 \tag{11}$$

Valid checking points were determined by using the following equations:

$$\begin{cases} x_t^2 + y_t^2 \le (R_1 + R_2)^2 \\ x_t \le R_1 \end{cases} \tag{12}$$

According to Eq. 10, Eq. 12 is shown below.

$$\begin{cases} (m_1 r_X + m_2 r_Y + m_3 r_Z + m_4)^2 \\ \quad + (a_{21} r_X + a_{22} r_Y + a_{23} r_Z - r_{0Y})^2 \le (R_1 + R_2)^2 \\ m_1 r_X + m_2 r_Y + m_3 r_Z + m_4 \le R_1 \end{cases} \tag{13}$$

The occurrence detection of rear gouging at the CCP is made through the valid checking points that satisfy Eq. 13.

2.3.3 Checking and avoidance of rear gouging

If all the valid checking points are below the bottom plane of the cutter, it implies there is little rear gouging. The z_t value of the valid checking point is used to check the occurrence of rear gouging. When z_t >0, the valid checking point is usually above the bottom plane of the cutter and results in rear gouging. The existing condition of the CCP being below the bottom plane of the cutter is given as follows:

$$z_t = n_1 r_X + n_2 r_Y + n_3 r_Z + n_4 \le 0 \tag{14}$$

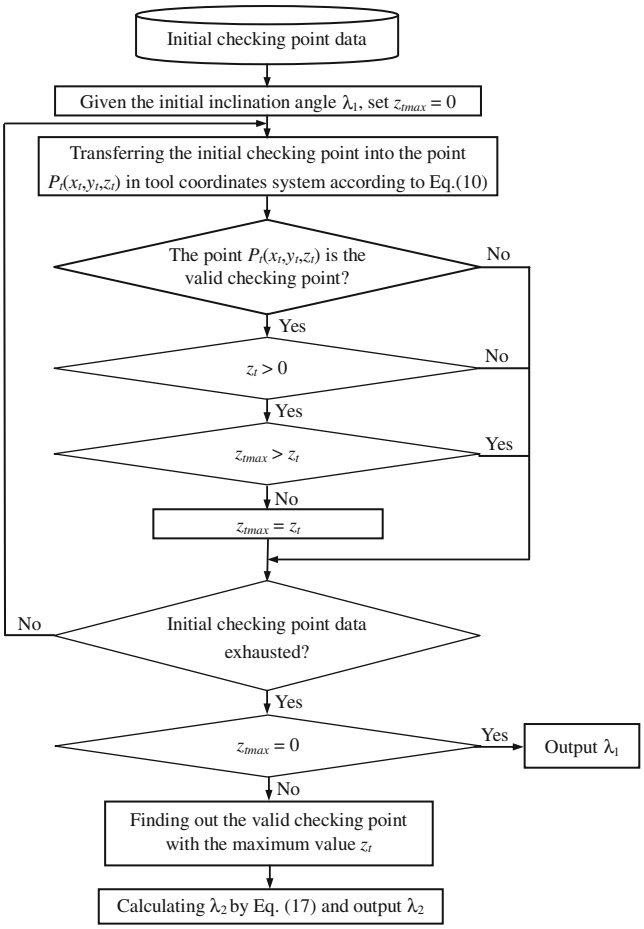

Fig. 5 A flow chart for detection and avoidance of rear gouging

Detection and avoidance of rear gouging can be achieved using the following steps:

1. Assumption that all values of z_t meet Eq. 14, then it indicates there is no occurrence of rear gouging at the CCP, and the initial tool inclination angle λ_1 is used as the final tool inclination angle.
2. It should be noted that there are some valid checking points that do not meet Eq. 14, therefore the maximum value of z_{tmax} needs to be selected from those checking points, where $z_{t\max} = \text{MAX}\{z_t | z_t > 0, .x_t^2 + y_t^2 \le (R_1 + R_2)^2, x_t \le R_1\}$.
3. Rear gouging can be avoided by increasing the initial inclination angle λ_1 until a valid checking point having the maximum value of z_{tmax} is on the bottom plane of the cutter. To make it clear, the proper inclination angle will enable z_{tmax} to equal to 0. The right inclination angle labeled as λ_2 can be obtained by these equations listed below.

$$\begin{cases} \sin^2\lambda_2 + \cos^2\lambda_2 = 1 \\ z_{t\,\max} = 0 \end{cases} \tag{15}$$

Equation 15 can be expressed also by using Eq. 10 as indicated below:

$$\begin{cases} \sin^2\lambda_2 + \cos^2\lambda_2 = 1 \\ A\sin\lambda_2 + B\cos\lambda_2 + R_2 = 0 \end{cases} \tag{16}$$

where,

$$A = [r_X \quad r_Y \quad r_Z \quad -1][a_{11} \quad a_{12} \quad a_{13} \quad r_{0X} + r_{0Y}]^{-1}$$
$$B = [r_X \quad r_Y \quad r_Z \quad -1][a_{31} \quad a_{32} \quad a_{33} \quad r_{0Z} + R_2]^{-1}$$

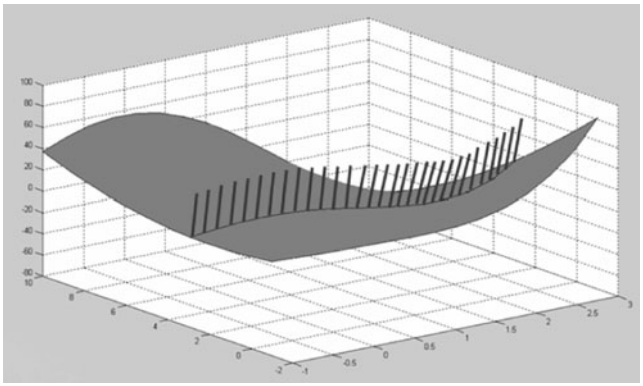

Fig. 7 Inclination variation of cutter along tool path curve

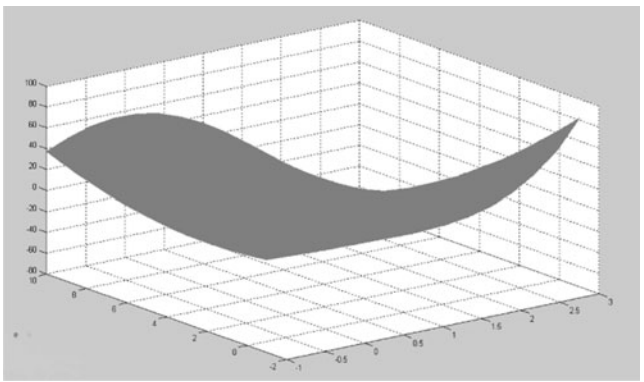

Fig. 6 A example of NURBS surface

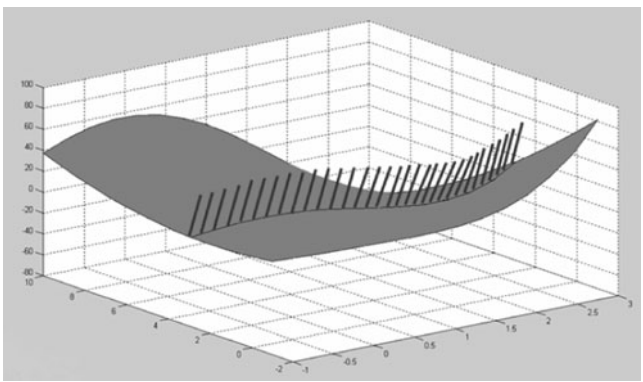

Fig. 8 Inclination variation of cutter during traditional machining

The final tool inclination angle λ_2 can be calculated from the following equation:

$$\lambda_2 = \sin^{-1}\left(\frac{-b+\sqrt{b^2-4ac}}{2a}\right) \tag{17}$$

where,

$$a = A^2 + B^2, b = 2AR_2, \text{ and } c = R_2^2 - B^2$$

Change of the tool inclination angle from λ_1 to λ_2 also eliminates the local curvature interference between the part surface and the cutter surface at the CCP due to a proportional increase in the minimum principal curvature of the cutter. See chart below for an in-depth explanation of the procedure for the detection and avoidance of cutter gouging as specified in Fig. 5.

3 An example

A nonuniform rational B spline (NURBS) surface was chosen to illustrate this method of detection and avoidance of cutter gouging as shown in Fig. 6. A traditional iso-parameter tool path is used to generate cutter contact curves and cutter location points. Machining error δ was set to 0.001 mm, enabling cutter contact curves to be discretized into the CCP allowing for the calculation of the maximum and minimum principal curvature of the NURBS for each individual CCP. Efficiency in calculation is improved through using the second order Taylor expansion of a NURBS surface to compute the first and second fundamental elements which are E, F, G, L, M, and N, respectively. The maximum and minimum principal curvature signs are used to decide the shape of the NURBS surface at each CCP. The maximum principal curvature $K_{\Sigma\max}$ of concave surface is worked out by Eq. 1 and is equal to 0.045.

Prior to testing, cutter radii must be firstly established. Initial cutter radii R_1 and R_2 are set to 6 and 4 mm, based on the maximum principal curvature $K_{\Sigma\max}$. Setting the value of λ_0 to 30°, $R_{2\min}$ to 2 mm, ΔR_1 to 0.2 mm, and ΔR_2 to 0.2 mm, the final sizes of cutter radii R_1 and R_2 were solved out by selection algorithm of cutter radius shown in Fig. 3, equaling to 6 mm for radius R_1 and 3.5 mm for radius R_2.

Once the cutter radii and CCP are known, a final cutter inclination angle can be found by this elimination method of cutter gouging as put forward in this article. Cutter gouging is avoided at the local and rear areas of every CCP by the final inclination angle. Figure 7 illustrates a variation tendency of cutter inclination angles that occur along one of the tool paths curve on the part surface.

Complex surfaces are made with the use of a five-axis CNC machine tool in most factories. To avoid cutter gouging during the machining, the conservative big cutter inclination angle is employed to eliminate local curvature interference at the CC point and rear interference. Figure 8 displays the variation tendency of the cutter inclination angle along one of the tool paths curve in a traditional application of the machining process. These differences by comparison of the two figures show that Fig. 7 has a smaller cutter inclination angle than Fig. 8 along the same tool path curve. Apparently, a smaller tool inclination angle application along the tool path curve is preferable to a large tool path interval to achieve the higher machining efficiency.

4 Conclusions

Gouging detection and avoidance technique has been presented for the five-axis machining of a complex surface with C^2 continuity using a fillet-end milling cutter. Initially, the part surface must be classified into conclave and convex shapes by the two signs representing the minimum and maximum principal curvature. Cutter radii size is selected by the exact curvature matching principle to avoid local curvature interference in every direction at the CCP on the concave surface. Rear gouging detection is performed by accurately judging the position of the each valid checking point relative to the bottom plane of the cutter. Generation of the checking area and checking points is completed by an algorithm based upon the square grid points. Compared with other algorithms for the detection and avoidance of cutter gouging, the method in this study proposed is more efficient and precise and it can be used in three-, four-, or five-axis CNC machining for producing good surface finish and high machining precision.

Acknowledgments This research was supported by the National Natural Science Foundation of China under grant no. 50805099 and the Top Young Academic Leaders of Higher Learning Institutions of Shanxi Province under grant no. 20091091 (TYAL). The authors would like to thank the anonymous reviewers for their valuable remarks and comments.

References

1. Kim BH, Chu CN (1994) Effect of cutter mark on surface roughness and scallop height in sculptured surface machining. Comput Aided Des 26(3):179–188
2. Yoon JH (2005) Fast toolpath generation by the iso-scallop height method for ball-end milling of sculptured surfaces. Int J Prod Res 43(23):4989–4998
3. Yoon JH (2007) Two-dimensional representation of machining geometry and tool path generation for ball-end milling of sculptured surfaces. Int J Prod Res 45(14):3151–3164
4. Li H, Feng HY (2004) An efficient five-axis machining of free-form surfaces with constant scallop height tool paths. Int J Prod Res 42(12):2403–2417

5. Than L, Jae-Woo L, Erik LJ, Bohez (2009) A new accurate curvature matching and optimal tool based five-axis machining algorithm. J Mech Sci Technol 23(10):2624–2634
6. Guillaume F, Gerard P (2010) Modeling of interferences during threads milling operation. Int J Adv Manuf Technol 49(1–4):41–51
7. Cha-Soo S, Kyungduck C, Yuan-Shin L (2003) Optimizing tool orientation for 5-axis machining by configuration-space search method. Computer-Aided Des 35(6):549–566
8. Chu CH, Chen GT (2006) Tool path planning for five-axis flank milling with developable surface approximation. Int J Adv Manuf Technol 29(7–8):707–713
9. Rao A, Sarma R (2000) On local gouging in five-axis sculptured surface machining using flat-end tools. Computer-Aided Des 32 (7):409–420
10. Mohammad JBF, Feng HY (2009) Effect of tool tilt angle on machining strip width in five-axis flat-end milling of free-form surfaces. Int J Adv Manuf Technol 44(3–4):211–222
11. Yu W, Tang XW (1999) Five-axis NC machining of sculptured surfaces. Int J Adv Manuf Technol 15(1):7–14
12. Mullins SH, Jensen CG, Anderson DC (1993) Scallop elimination based on precise five-axis tool placement, orientation, and step-over calculations. ASME Adv Des Autom 65(2):535–544
13. Jensen CG, Anderson DC (1992) Accurate tool placement and orientation for finish surface machining. ASME Concurr Eng 59:127–145
14. Jensen CG, Mulkay EL, Simpson TS (1995) A practical implementation of curvature matched machining for complex geometric objects. ASME Concurr Prod Process Eng 85:1–14
15. Lee YS, Ji H (1997) Surface interrogation and machining strip evaluation for 5-axis CNC die and mold machining. Int J Prod Res 35(1):225–252
16. Lee YS, Chang TC (1996) Automatic cutter selection for five-axis sculptured surface machining. Int J Prod Res 34(4):977–998
17. Chen LG, Cheng JW, Wang YZ (2008) Tool path generation argorithm for five-axis NC machining with a toroidal cutter. Chin J Mech Eng 44(3):205–212
18. Lee YS (1997) Admissible tool orientation control of gouging avoidance for 5-axis complex surface machining. Computer-Aided Des 29(7):507–521
19. Wu BH, Luo M, Zhang Y, Li S, Zhang DH (2008) Advances in tool path planning techniques for 5-axis machining of sculptured surfaces. Chin J Mech Eng 44(10):9–18
20. Hosseinkhani Y, Akbari J, Vafaeesefat A (2007) Penetration-elimination method for five-axis CNC machining of sculptured surfaces. Int J Mach Tool Manuf 47(10):1625–1635
21. Jensen CG, Red WE, Pi J (2002) Tool selection for five-axis curvature matched machining. Comput-Aided Des 34(3):251–266
22. Zhong JL, Mi NS, Yu YD (1999) Research on algorithm of automatic generation of interference-free cutter location path for NC machining of freeform surfaces with flat-end cutters. Chin J Mech Eng 35(6):93–97
23. Chen LW, Ceng JJ, Li GW (2000) Tool path interference elimination algorithm of sculptured surfaces. J Southeast Univ 30(6):44–47, Natural Science Edition
24. Ahmet C, Ali U (2010) A novel iso-scallop tool-path generation for efficient five-axis machining of free-form surfaces. Int J Adv Manuf Technol 51(9–12):1083–1098
25. Jensen CG, Anderson DC (1993) Accurate tool placement and orientation for finish surface machining. J Des Manuf 3(4):251–261
26. Chiou CJ, Lee YS (2005) Optimal tool orientation for five-axis tool-end machining by swept envelope approach. ASME J Manuf Sci Eng 127(4):810–818
27. Anotaipaiboon W, Makhanov SS (2005) Tool path generation for five-axis NC machining using adaptive space-filling curves. Int J Prod Res 43(8):1643–1665